High Time Resolution Astronomy
Or High Speed Photometry

Gary A. Vander Haagen
Stonegate Observatory
825 Stonegate Rd, Ann Arbor, MI 48103
garyvh2@gmail.com

Abstract

High Time Resolution Astronomy (HTRA) or High Speed Photometry offers opportunity to investigate phenomena that take place at timescales too fast for standard CCD imaging. Phenomena that occur within fractional-seconds to sub-millisecond timescales have been largely overlooked until recently due to technology `limitations and/or research priorities in other areas. Discussed within the 1-second to millisecond range are flares, oscillations, quasi-periodic oscillations (QPOs), and lunar occultations. A Silicon Photomultiplier (SPM) detector with associated pulse amplifier and high-speed data acquisition system were used to capture stellar intensities at rates up to 1000 samples/sec on stars to 8 V-mag. Results on YY Gem flares, exploratory searches for oscillations on AW Uma, BM Ori, and X Per, and lunar occultations are discussed along with data reductions techniques. Opportunity for future study is also discussed.

1. Introduction

Our fascination with solar the system, star systems and their evolution, asteroid tracking, rotation, sizes, and composition as a few examples have led us to fainter and fainter objects, larger optics, and longer exposures. With longer exposures, events that take place in the fractional-second to millisecond timescale are averaged and lost.

Interest in this area opens up a whole new range of possible explorations. High speed photometry or high time resolution astronomy (HTRA) can fill an area of scientific exploration that complements conventional CCD imaging and offers unique insight into relatively unexplored areas. "Stellar Oscillation and Occultations", Richichi (2010), presents a good overview of how HTRA augments astronomical research. Figure 1 shows research areas versus timescale and the regions of study. Pulsars, oscillations, quasi-periodic oscillations (QPOs), and occultations push the millisecond and beyond range. These represent significant equipment challenges requiring very fast and sensitive photo detectors and larger aperture optics for 8-9 magnitude and beyond. In addition, with data rates in the kilohertz range there are challenges in coping with the storage and analysis of the data. With intensity sampling at 1000 samples/sec a two-hour data collection run generates 7.2 million data points for storage and subsequent analysis.

For the slower oscillations, transits, flares, and flicker events, data rates in the 10 to 100 Hz range still present the same equipment challenges but offer opportunity for the study of fainter objects. The previously cited Stellar Oscillation and Occultation article presents numerous examples for study in these areas.
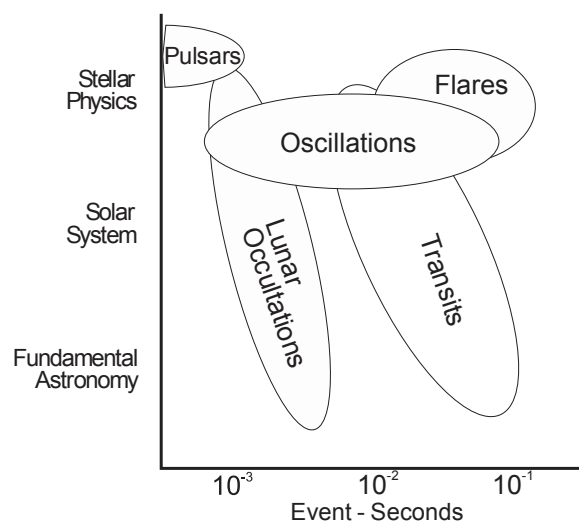

Figure 1, research opportunities at various timescales, facsimile reproduced by permission from A. Richichi

The tradeoff between sampling rates and S/N is shown in Figure 2 for sampling rates of 10, 100, and 1000

samples/sec. This graph shows ideal conditions using a clear filter with minimal scintillation noise. The telescope has a 17" aperture and a silicon photomultiplier detector (SPM) with an internal gain in excess of 10^6. At 1000 samples/sec the measurement limit is approximately 8th magnitude.
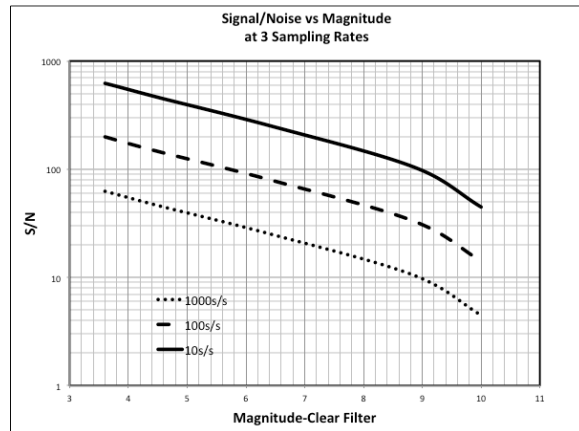

Figure 2, S/N versus magnitude for 3-sampling rates with clear filter and low scintillation noise

When pursuing fast events bandwidth (BW) is limited by our sampling rate. To avoid aliasing during analysis, the sampling rate (f_s) must exceed the Nyquist rate (f_n),

$$f_s > f_n, \text{ where } f_n = 2BW$$

Or, for a BW of 1000 Hz the sampling rate must be greater than 2000 Hz. Literature places a number of the oscillations events in the mHz-1900 Hz region for x-ray binaries (XB), Warner (2008). Targeting of the 1900 Hz oscillation dictates a minimum sampling rates of 3800 samples/sec thereby limiting objects to approximately 6th magnitude or brighter for 14-17" scopes. For slightly less demanding lunar occultation studies a resolution of 1-3 milliseconds is required for diffraction fringe capture. This places sampling rates in the 300 to 1000 samples/sec range. These rates and the slightly slower flares and flickers can push the upper limit to as high as 10th magnitude under ideal conditions.

With an practical upper limit of 9th magnitude the initial candidates for fast event studies are shown in Figure 3.

2. The Optical Train for High Speed Photometry

Key components of the optical system include a telescope with 10" or greater aperture, a fast response detector system with internal gain, data acquisition system and analysis software.

| Target	Type	Visual Magnitude
X Per	HMXB Pulsar	6.7
AW Uma	CV	6.9
BM Ori	EB, X-ray source	8
YY Gem	EB, X-ray source	9.8
RZ Cas	EB, X-ray source	6.2
Moon Occultations	Single & double stars	8 or brighter

Figure 3, HTRA study targets

The detector represents the biggest challenge for HTRA. While there are several CCD cameras available with internal gain (electron multiplication) they are expensive and do not provide the S/N of photomultiplier type sensors. However, they do provide a mechanism for obtaining a reference star and using more conventional data reduction techniques. The discussion presented in "The Silicon Photomultiplier for High Speed Photometry", Vander Haagen (2011), provides and overview of numerous sensor types and their performance. The characteristics that make the Silicon Photomultiplier (SPM) most attractive are high internal gain (10^{6+}), good noise performance, wide bandwidth and insensitivity to overloading, troublesome with conventional vacuum photomultipliers.

The SPM used was manufactured by sensL, sensL (2012). Figure 4 shows both the unpackaged sensor along with it fully enclosed and cooled and attached to a nose piece with filter and f-stop. The output of the SPM is millivolt level pulses at rates up 10 MHz depending on the equivalent photon count per second, one photon per count. These low voltage pulses are fed to a wideband pulse amplifier to provide a logic level signal for the data acquisition system. The amplifier provides a voltage gain of 2500 at a bandwidth of 10MHz necessary for undistorted photon pulse counts. This is a higher performance version of the previously used amplifier. The new amplifier provides about double the BW and greater stability to temperature and input-output loading changes. A schematic of the circuit may be requested from the author.

The initial optical train used had a field of view of 80 arcseconds. The configuration used a video camera for alignment and relied on accurate tracking from the mount for extented periods. Without guiding, tracking errors were excessive for multiple-hour data collection runs. The optical train was modified to improve ease of initial alignment and provide continuous autoguiding. The modified optical train is shown in Figure 5
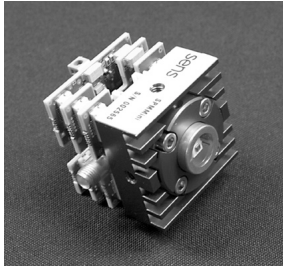
a.
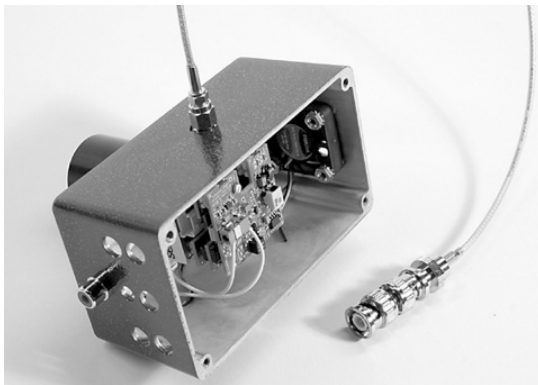
b.

Figure 4a, SPM module. Figure 4b, SPM module packaged with cooling fan, nosepiece, f-stop and filter. A cooling fan is required to keep the thermoelectric cooler operating at 30 C below ambient.
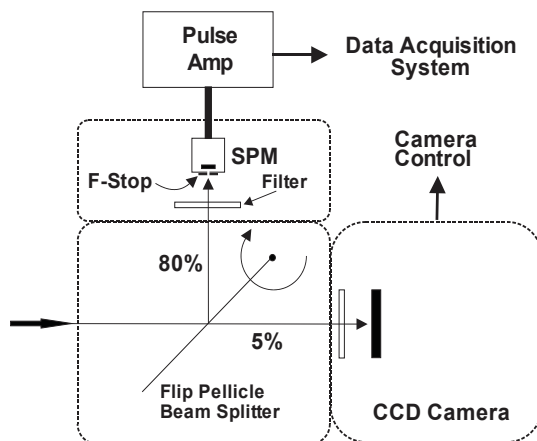

Figure 5, optical train with flip pellicle beam splitter, SPM module, and CCD camera for alignment and guiding

The light enters and strikes a 5-micron pellicle beam splitter, National Photocolor (2012).

Approximately 80% of the light is reflected 90^0, passing through the optical filter, f-stop, and onto the SPM. The CCD camera for initial set up and autoguiding uses the 5% transmitted light. A software controlled servo motor positions the pellicle for either beam splitting mode or 100% pass through for normal CCD camera operation. The optical train has demonstrated easy initial alignment and guiding for the long data collection runs.

The f-stop most generally used was 750μm diameter providing a field of 57-arcseconds. A smaller 400μm diameter f-stop was required for lunar occultation work.

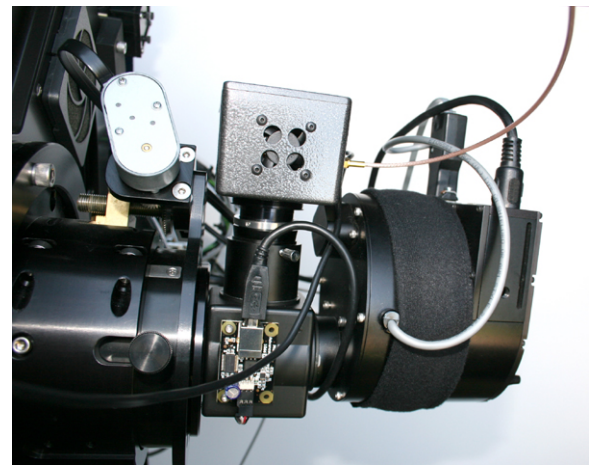The full optical train is shown in Figure 6 mounted on the 17" PlaneWave scope.

Figure 6, optical train showing SPM and CCD camera attached to software controlled pellicle beam splitter

3. High Speed Data Acquisition and Analysis

The basic data collection sequence will operate without a reference star. Since we are operating with a single pixel camera there is no option for a reference without adding a second complete optical train with associated equipment and alignment issues. In addition, the two data streams are generally correlated in real time. Such a setup is described in Uthas (2005) and is generally not necessary for the higher frequency data particularly where data is at a frequency substantially higher than the scintillation noise. An alternative calibration option will be discussed in Section 7.

The data acquisition system used was from, Measurement Computing Corporation (2012), a DaqBoard/1000 series data acquisition board. The PCI board takes one PC slot with the data inputted through a standalone connection board. Important feature of the data acquisition system include:

1. Easy connection and use with PC at lowest system cost
2. Bandwidth capability to at least 8×10^6-photon integration counts per second.
3. Ability to totalize counts over any period; μseconds to seconds
4. Ability to trigger data collection on a count, count rate or analog event and employ a caching technique for pre-trigger data capture
5. Integrated DaqView software for real time data storage and review of events

The integrated DaqView software met all the data acquisition requirements but did not include a suite of digital signal processing (DSP) subroutines for Fourier transforms, power spectral density, filtering, smoothing, etc. Sigview 2.3, a DSP package by SignalLab (2012) had the required capability. Sigview has an intuitive structure and easily imports ANSI data from the MC data acquisition system. This software provides capability for all the filtering modes such as low pass, high pass, band pass, fast Fourier transforms (FFT), spectrograms, statistical analysis, amplitude and frequency measurements, adding and parsing of data runs, etc. This capability helps to reduce the dependency on a secondary reference star, to some extent, as will be described later.

4. Exploratory Look at Rapid Events in Eclipsing and X-ray Binaries

The primary interest of this study is the stellar physics events as shown in Figure 1. The focus will be on cataclysmic variables (CVs) particularly X-Ray binaries (XB) exhibiting QPO or suspected optical oscillations. Current models suggest magnetically controlled accretion onto a rapidly rotating equatorial belt of gas. These energetic events may generate RF, X-Rays, and occasionally modulate emitted light in the form of oscillations or QPOs with signatures varying widely, Uthas (2005) and Warner (2008).

Flares are well known events for our Sun and other stars and CVs with strong magnetic fields at their surfaces. An energetic flare can produce luminosity increases of many orders of magnitude on time scales of seconds to days. Flickering is a smaller outburst of a few tenths of a magnitude over a much shorter time, generally seconds to minutes.

Be it oscillations, flares, or flickering events they occur rapidly such that detailed high-speed data is necessary for capture. These data are used to develop or validate models for the stellar systems. For the oscillations, target frequencies range from 40-2000 Hz placing these frequencies generally beyond the worst of the scintillation noise. Targeted will be those stars or star systems with suspected or verified events and at data rates necessary to capture the oscillation. The limiting factor will be target brightness necessary to support the fast exposures. The data will be captured at data rates as high as possible in segments of 10^6 data points for each file. The data acquisition system supports continuous data collection but limits the file size for analysis purposes. The prime tool for identifying the oscillations will be the Fourier transform power spectral density (PSD) of the amplitude-time data and the Spectrogram or a time sequence PSD showing where in time the frequency occurred.

For flares and flickering events the time domain data will be reviewed directly or bandpass filtering and/or resampling of the data will be used to reduce the high frequency variations. The same segmenting of data will limit individual files to 10^6 points.

Data collection objectives will be exploratory in nature:
1. Confirming the range of data gathering of both magnitude and BW.
2. Learning to separate noise from stellar information focusing on XB with known oscillations in the X-Ray spectrum and "suspect" in the optical.
3. Refining equipment and procedures for improve results.
4. Firming up a plan for next steps including working with a researcher.

4.1 AW UMa

AW UMa is a cataclysmic variable; HMXB targeted because of its general classification and previous interest by other researchers. The first run of AW UMa was at 200 sample/sec and the initial look at the data generated considerable excitement. Figure 7 shows an expanded section of the 3600-second run.
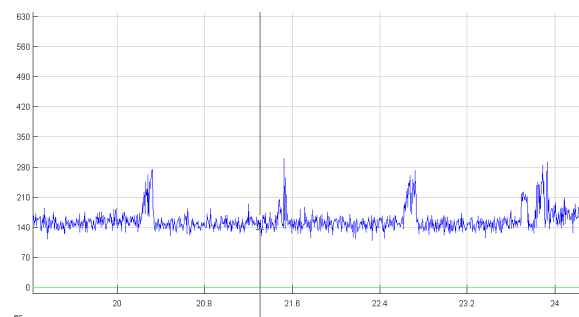

Figure 7, AW Uma data at 200 samples/sec, 7-second section noting periodic pulses

These periodic pulses were found later to originate from an open ground on a coax connection. Considerable attention is necessary to address noise

across the full spectrum prior to any data collection. Flipping the pellicle to the pass through position blocks the sensor and helps to confirm proper noise performance. This step was accidentally omitted prior to this run. Three additional 1-hour runs were completed on a second night. No high frequency components were detected.

4.2 X Per

X Per is a HMXB, Pulsar, and gamma-ray source and suitable classification for high frequency activity. The 6.7 V magnitude allowed for data collection at 1000 samples/sec. All runs were with Astrodon Johnson-Cousins blue filters. Run #1 on 2012-03-07 was 6-segments of 1-million data points each. The files are seamless from one to the next so no data is lost. Run #2 on 2012-03-09 was 8-segments of 1-million points each. A PSD of a typical run is shown in Figure 8.
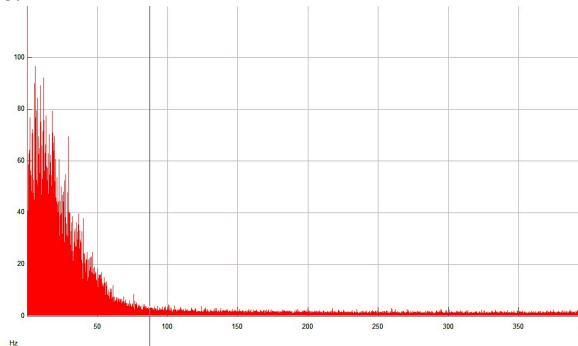

Figure 8, X Per PSD data at 1000 samples/sec, typical spectra with no high frequency components to 500 Hz

Another X Per run occurred on 2010-03-15; 10-segments of 1-million points each. A composite of the first 4-segments is shown in Figure 9.
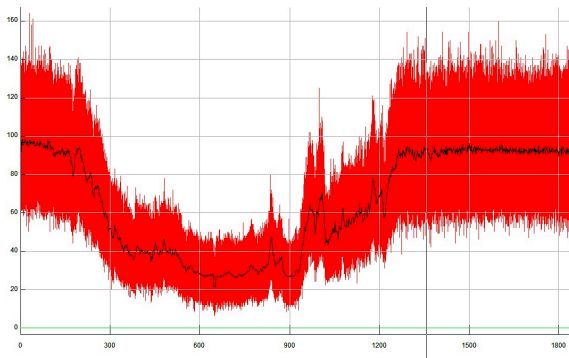

Figure 9, X Per data at 1000 samples/sec, composite of 4-segments. The smooth data were resampled at 1-sample/sec

The data encompasses a short eclipse that seems unreported in the literature. The cloud sensing system showed no change in the sky condition during the period. Note also what appear to be small flares during the eclipse. A PSD of the flare section is shown in Figure 10.
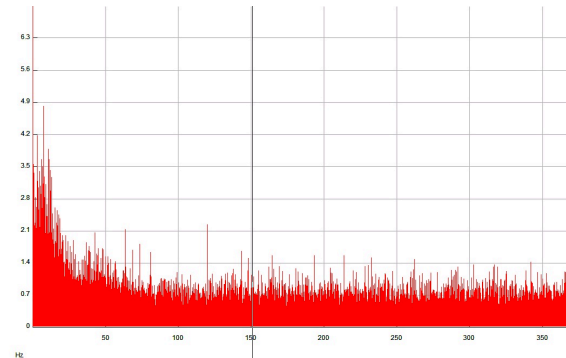

Figure 10, X Per PSD of flare section

Figure 10 shows no identifiable high frequency components. However, on run #6 there was an identifiable peak at 383 Hz as shown in Figure 11, a potential QPO.
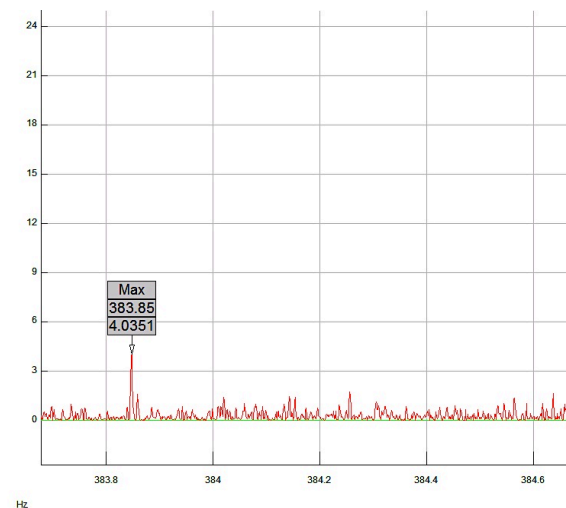

Figure 11, X Per PSD data at 1000 samples/sec, run #6; a potential QPO at 383.85 Hz

A very high amplitude peak was detected during segment 5. With the mean count running at approximately 100, just after 306 seconds on segment 5 the counts peaked over 3200. Figure 12 shows this event. The signal profile does not match a flash tube typical of emergency vehicles. No clouds were present for possible lightening flash. A possible explanation is a stray emergency vehicle rotating light flash from a nearby road. These data will be investigated further.
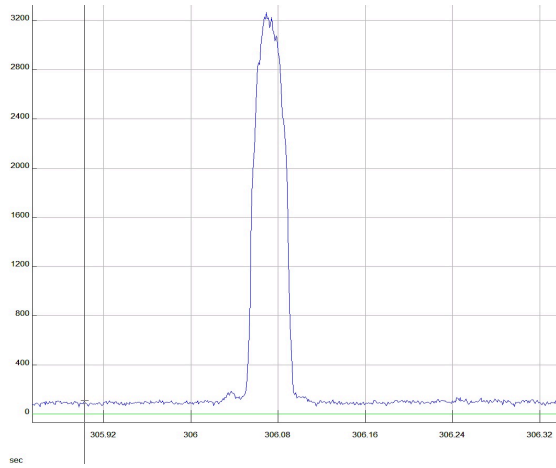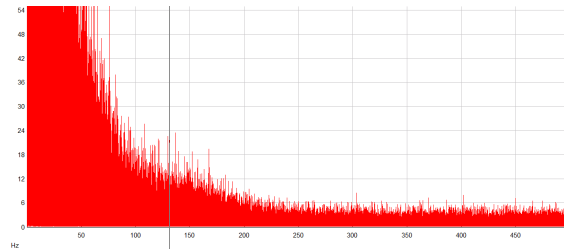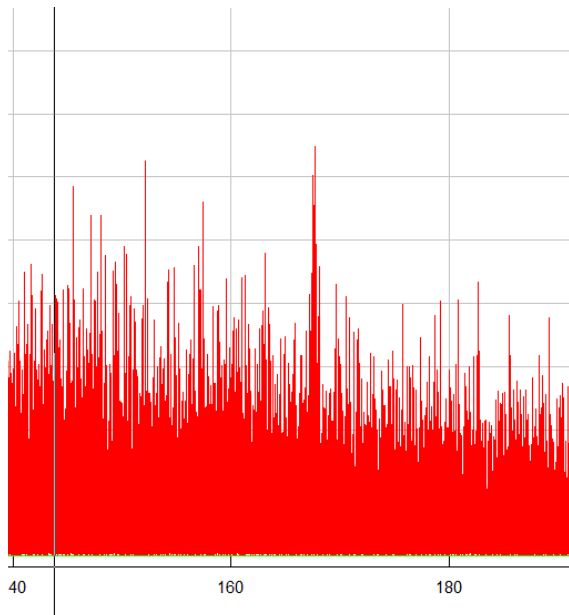
Figure 12, X Per data for segment 5 showing very high peaking near 306 seconds
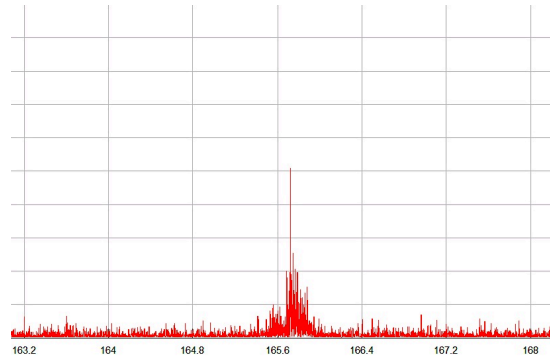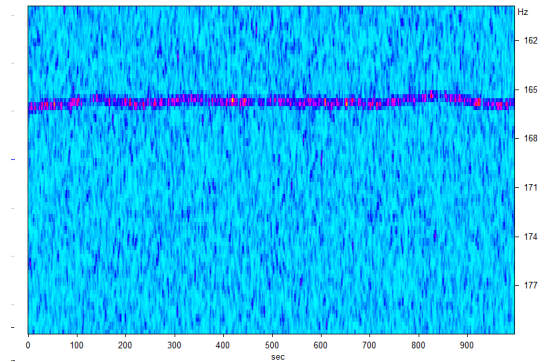

a.

b.

Figure 13, BM Ori PSD data; Figure 13a. full 500 Hz BW and Figure 13b. region around 167.6 Hz

a.

b.

Figure 14, BM Ori PSD and Spectrogram; Figure 13a. region around 166 Hz and Figure 13b. Spectrogram showing the distribution of the 166 Hz oscillation over the 1000- seconds. The Spectrogram's brighter spots indicate higher concentration of the oscillation. Note small frequency change over the 1000-second period.

With so little data available at these data rates it is difficult to validate and exciting to see what is captured on each nights runs.

4.3 BM Ori

BM Ori is an eclipsing binary and X-Ray source with good sky position for long runs. The EB was studied two nights 2012-03-17/20 at 1000 samples/sec. On the first run PSD analysis showed peaking of data at 167 Hz on three of the 1-million data point segments. Figure 13 shows both the full PSD and a section focused on 168.6 Hz. The same peak occurred in all the other segments of this run. On 2102-03-20 another run was completed with 8-segments of 1-million points each. The data looked similar with the 167 Hz components showing in all 8-segments. Figure 14 shows the PSD and a spectrogram of segment 8.

4.4 YY Gem

As a clouded-in participant of the YY Gem photometric team, this star generated considerable interest for future study of its active flares. YY Gem

is an M dwarf eclipsing binary and known flare star. With it's 9.8 V magnitude, data was collected at 200 samples/sec giving a BW of 100 Hz. Data were collected for a 2-hour and 6-hour run on two nights. Figure 15 shows the full 3600 seconds of data for 2012-03-13.
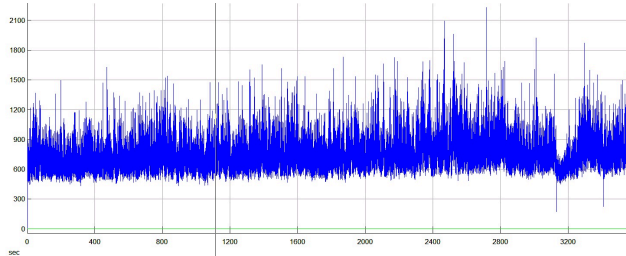

Figure 15, YY Gem data for 2012-02-13, blue filter, 200 samples/sec, with 3600-second trace

With data compressed it looks noisier than would be expected. However, with an average count of 600+ the S/N was 15 and acceptable. The PSD of the same data is shown in Figure 16.
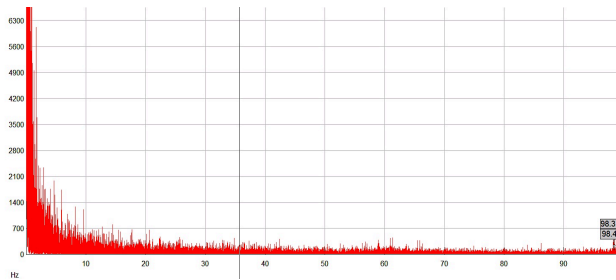

Figure 16, YY Gem PSD data for 2012-02-13, blue filter, 200 samples/sec, BW = 100Hz

The FFT shows strong components below 5 Hz and reaching background levels by 25 Hz. There were two low level components at 65 and 98 Hz at very low power density.
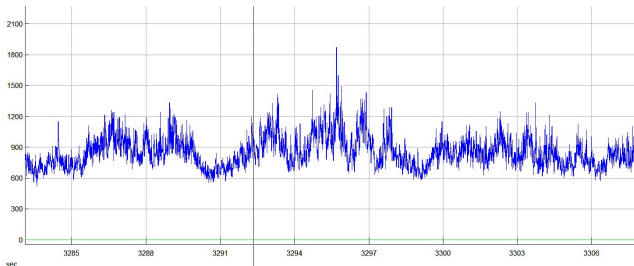

Figure 17, YY Gem flicker event

Figure 17 shows a flicker event with a total duration of less than 10 seconds at approximately a magnitude brightening at the peak. This star warrants longer data runs through multiple eclipses (0.814 days

primary) to increase the chase of flare and flicker capture.

5. Lunar Occultations; a High Accuracy Measurement Tool

The Moon has held all those studying the heavens for thousands of years in great fascination. However, it has only been in the last 60 years that the Moon's predictable and known apparent angular rate of motion (0.4"/sec) and accurately known distance has been augmented by a well-understood occultation process, Nather, Evans, and McCants (1970a,b). With good physical data, timing to 1-millisecond, and a detailed model of the diffraction pattern created by the lunar edge, occulted object angular diameters and double star separations can be calculated with high accuracy, Richichi (2005).

The limitation of this tool is that the lunar occultations cover about 10% of the sky area over its 18.6-year cycle. Furthermore, many occultations occur during the day, are reappearances and require accurate off axes guiding for the hour or more the star is behind the Moon, and the light scattered from the illuminated portion has to be sufficiently low to yield adequate S/N. And, then there are still sky conditions and the instrumentation. The author recommends reading a good primer "Lunar Occultations", Blow (1983), that sets the stage well. "Combining optical Interferometry with Lunar Occultations", Richichi (2004), is also very informative. With all these difficulties lunar occultations still present an exciting challenge and area for accurate measurement of star diameters and separations using HTRA techniques.

The lunar occultation sequence can be seen in Figure 18 where a moving diffraction pattern is generated on the earth's surface by the star prior to the geometric shadow. The pattern and shadow is moving at approximately 750 meters/sec dependent upon the limb contact angle. To illustrate a simple diffraction pattern $F(w)$ for a monochromatic point-source the intensity:

$$F(w)=1/2\left[\left(\frac{1}{2}+S(w)\right)^2+\left(\frac{1}{2}+C(w)\right)^2\right]$$

where $S(w)$ and $C(w)$ are the Fresnel sine and cosine integrals and

$$w = x\sqrt{2/\lambda D}$$

so the diffraction intensity is a function of both the wavelength (λ) of observation and the lunar distance D. The Fresnel integrals can be calculated with a

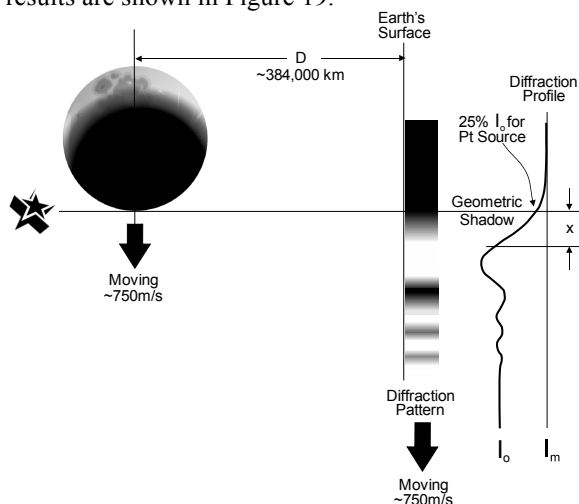MathCad type program or using Keisan (2012). The results are shown in Figure 19.

Figure 18, lunar occultation of star showing moving diffraction pattern on earth's surface
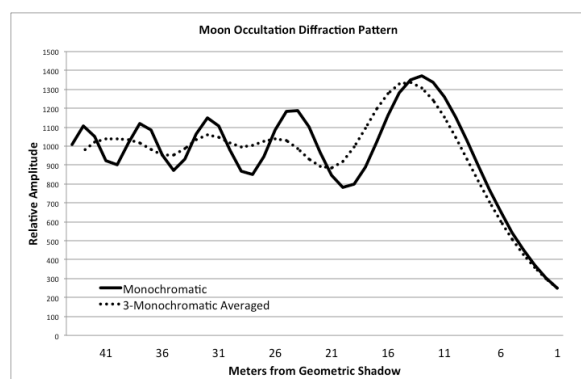

Figure 19, single and multiple colors diffraction patterns formed on earth's surface, distance in meters from the geometric shadow

The solid line shows a monochromatic pattern for source at 430 nm. Clearly defined interference fringes exist past 41 meters from the geometric shadow. With the fringes moving at 750m/s the fringe rate is 0.75m/millisecond or the first fringe passes in about 12 milliseconds. Since our stars are anything but monochromatic we average three monochromatic wavelengths, to keep the math simple, and get the dotted interference pattern. Note the significant blurring of the fringes. It only gets worse as we integrate all the fringes over the BW of a typical narrow band filter and increase the diameter of the source to something finite. A good set of pictorials illustrating the effects of wavelength, BW, and star diameter is presented by Richmond (2005).

Nather and Evans (1970) developed one of the first diffraction models of the occultation event leading to more than two decades of refinements. A least squares fit to the data is made using model parameters such as star brightness profile, sky background, detector and filter response, integration time, Moon's physical parameters, etc. The stars diameter is an additional parameter to be varied to find the best chi-squared fit of the diffraction pattern to the data. A further refinement of the least squares model came with the "composed algorithm" (CAL), Richichi (1989), which incorporates an iterative algorithm to select the "most likely" brightness profile of the source thereby yielding correct solutions over a much wider range of noise levels. Researchers have reported angular diameters to 0.5% uncertainty using the CAL approach, Richichi (2005). In my brief contact with researchers these models are not available for general use and require collaboration with the researcher. With good models and millisecond data, a measurement range in angular diameters/separation from 2 to 300 milli-arcsecond (MAS) is possible, Richichi (2012).

As a simple example of how the fringe analysis process works using only one element of the diffraction profile, Richmond (2005), presents a simulation of a uniform circular disk on the fringe pattern. Figure 20 estimates the angular size of a disk based on the height ratio of the first fringe, $I_{fringe\ peak}/I_o$. For a point source the ratio is 1.31. For a 20 MAS diameter the ratio is 1.08.
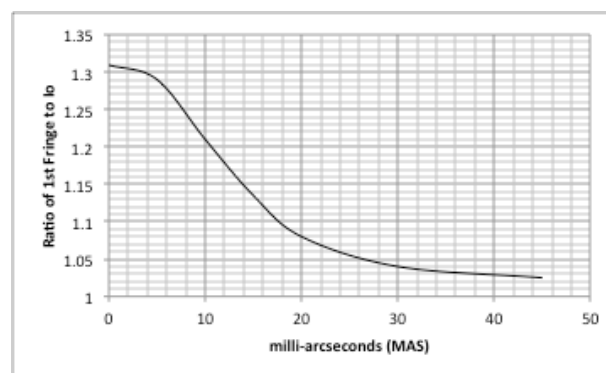

Figure 20, Angular size of a disk using only the ratio of first fringe height to steady state I_o

As seen this relies on only one characteristic of the data's profile and provides limited utility.

The video occultation measurement software LiMovie, Miyashita (2008), offers a graphing and diffraction matching routine. To date it has not been possible to use non-video data as a source for this program.

Two excellent references for lunar occultation predictions include: The International Occultation and Timing Association, IOTA (2012) and the Dutch Occultation Association with their Lunar Occultation

Workbench, DOA (2012). The Lunar Occultation Workbench (LOW) was found particularly user friendly and included many helpful cross-references.

Initial occultation data collection using a $750\mu m$ f-stop proved unsuccessful for a 7.05 V-mag star due to excessive dark limb illumination of the field. A second $150\mu m$ f-stop, 11 arcseconds field, proved nearly impossible to align and focus. Use of the $150\mu m$ diameter pinhole required a precision focuser in the SPM path, which could not be accommodated due to insufficient optical path length. A compromise $400\mu m$ f-stop, 30 arcseconds field, gave acceptable S/N for lunar phases to around 50% and 6^+ magnitude. Further work is necessary to determine the range of illumination and star magnitudes for the two smaller pinholes.

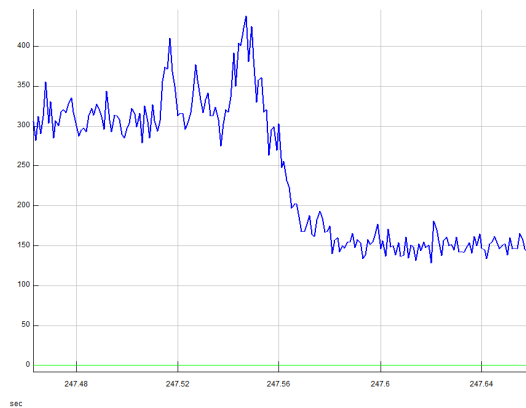Occultation of XZ-5588, 53 Tauri, SAO-76548, a 5.5 V-mag star is shown in Figure 21.

Figure 21, occultation of XZ-5588 at 1000 samples/sec using a blue J-C filter exhibiting 3-diffraction fringes
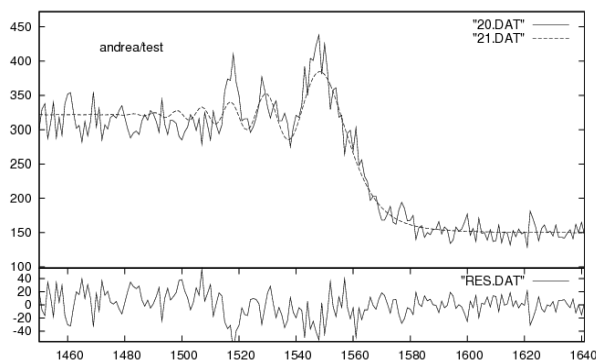

Figure 22, occultation of XZ-5588 with point source diffraction pattern shown (dotted) as determined by the CAL model, first trial

Using the first fringe ratio of 410/310 counts = 1.32, Figure 20 would place the star angular diameter at a point source or too small to be measured. A large amount of uncertainty results in this calculation due to the curves irregularity and simplicity of the model.

A CAL diffraction model was run on XZ-5588 data with an estimate of the SPM system parameters. The model found a point source assumption provided a good data fit with chi-squared of 0.97. The SPM system parameters are being reviewed and the model rerun to confirm the stars angular diameter.

Targets for Additional Study	Type	Visual Magnitude
1. X Per	HMXB Pulsar	6.7
2. AW Uma	CV	6.9
3. CygX-1	HMXB	8.9
4. YY Gem	EB, X-ray source	9.8
5. Vela X-1	XB	6.9
6. RZ Cas	EB, X-ray source	6.2
7. Lunar Occultations	Single & double star detection and measurement	8 or brighter

Figure 22, candidates for future HTRA study

6. Future Study Opportunities

The X-Ray binaries and cataclysmic variables are candidates that exhibit short or even extended periods of rapid variability in both the RF and the optical spectrum. Star systems such as Cygnus X-1 have exhibited modulation at frequencies in the 100 to 1300 Hz frequency range. This remains an opportunity for work in late summer and early fall when at its highest altitude. Vela X-1, HD77581, is another candidate for lower latitude study. Detection of these signals are challenging due to their low intensity, high frequency, and unpredictable occurrence. A study by Uthas (2005) and summary by Warner (2008) give some insight into this very interesting study group.

Flaring stars such as YY Gem are exciting study opportunities and allow for higher magnitude targets with sampling rates as low as 10 samples/sec.

The website ephemerides, Kreiner (2004), are excellent for identifying EB targets and timing as is the AAVSO (2012) for observing campaigns, descriptions of star types and their characteristics, classifications, outbreaks, data, charts, etc.

Occultations are a source of major interest at the higher sampling rates. The International Occultation and Timing Association, IOTA (2012) provides targets, technical assistance, and a depository for data.

7. Discussion and Conclusions

The SPM proved a capable detector for photon counting, high-speed photometric study. The use of the flip pellicle and capability for continuous guiding made set up easy and long term data acquisition possible without intervention. A setup modification using a helical focuser in the SPM's optical path would improve focusing for the smaller f-stop apertures. The focuser would also greatly reduce the wobble and misalignment that accompanies the sliding-tube focusing technique used. Field stops of 750, 400, and 150μm proved a reasonable choice. Modification of the optical train for quick change and registration of the f-stops would significantly reduce down time.

The absence of a reference star is problematic when lower frequency phenomena are investigated, e.g., flares, eclipses. One solution is use of the intensity data from the guide star as a reference. These data could be easily stored on one of the extra channels of the data acquisition system and used to eliminate the slower variability from atmospheric transmission changes occurring over periods of seconds.

Considering the 5-study objectives:
1. Confirm the range of data gathering of both magnitude and BW.

Sampling rates to 1000 samples/sec were possible to 8th magnitude providing the filter used matched the spectral characteristics of the target. A magnitude dimmer is possible without a filter. For brighter targets sampling rates to 10,000 samples/sec are possible.

2. Learn to separate noise from stellar information focusing on XB with known oscillations in the X-Ray spectrum and "suspect" in the optical.

Stellar oscillations were found on X Per at 383.86 Hz, and on BM Ori at 166-7 Hz, possible QPOs. No literature confirmation was found for these frequencies. Use of digital filtering and FFT processing easily separates these signals from the lower frequency scintillation noise. Attention must be given at all times for elimination of system noise from ground loops, other electronic equipment, and optical sources visible to the sensor.

3. Refine equipment and procedures for improve results.

Changes to the optical path for better initial alignment and tracking were successful.

4. Confirm the capability for data collection on lunar occultation events and processing of data.

The lunar occultation data for XZ-5588 was analyzed with the CAL model and found to be an unresolvable point source at high confidence.

5. Firm up plans for next steps including working with a researcher.

Identification of a researcher for collaboration on HTRA in high frequency oscillations and\or flaring is underway. Additional data collection on lunar occultations will also be pursued.

8. Acknowledgements

References

AAVSO (2012). American Association of Variable Star Observers. http://www.aavso.org/

Blow, G.L. (1983). Lunar Occultations. *Solar System Photometry Handbook*, Genet, R. M., pp. 9-1 to 9-25.

DOA (2012). The Dutch Occultation Association. Lunar Occultation Workbench, LOW Software v. 4.1. http://www.doa-site.nl/

IOTA (2012). International Occultation and Timing Association. http://lunar-occultations.com/iota/iotandx.htm

Keisan (2012). High accuracy scientific calculations. http://keisan.casio.com/has10/SpecExec.cgi?id=system/2006/1180573477

Kreiner, J.M. (2004). Up-to date linear elements of close binaries. *Acta Astronomica,* vol. 54, pp. 207-210, http://www.as.up.krakow.pl/ephem/

Measurement Computing Corporation (2012). IOTech Data Acquisition Equipment. http://www.mccdaq.com/products/daqboard_series.aspx

Menke, J., Vander Haagen, G.A. (2010). High speed photometry detection and analysis techniques. *The Alt-Az Initiative,* Genet, R.M., Johnson, J.M., and Wallen, V., pp. 443-469.

Miyashita, K. (2008). LiMovie software for video analysis of occultation events. http://www005.upp.so-net.ne.jp/k_miyash/occ02/limovie_en.html

Nather, R. E., Evans, D. S. (1970a). Astronomical Journal v. 75, pp. 575-582

Nather, R. E., McCants, M. M., (1970b). Photoelectric Measurement of Lunar Occultations IV. Data Analysis. Astronomical Journal v. 75, pp. 963-968.

National Photocolor, Inc. (2012). Manufacturers of pellicle mirrors and beam splitters. http://www.nationalphotocolor.com/specs.html

Richichi, A. (1989). Model Independent Retrieval of Brightness Profiles from Lunar Occultation Light Curves in the Near Infrared Domain. Astronomy and Astrophysics, 226, pp. 366-372.

Richichi, A. (2004). Combining Optical Interferometry with Lunar Occultations. ASP Conference Series, Vol. 318, pp. 148-156.

Richichi, A., Roccatagliata, V. 2005. Aldebaran's angular diameter: How well do we know it? A & A 433, pp. 305-312.

Richichi, A. (2010). Stellar Oscillations and Occultations. High Time Resolution Astrophysics IV. Agios Nikolaos, Crete, Greece, May 5, 2010.

Richichi, A. (2012). Personal communications.

Richmond, M. (2005). Diffraction effects during lunar occultations. http://spiff.rit.edu/richmond/occult/bessel/bessel.html

sensL Technologies Ltd. (2012). Manufacturers of SPMs. http://sensl.com/products/silicon-photomultipliers/

SignalLab (2012). Sigview 2.3 software for DSP applications, http://www.sigview.com/index.htm

Soydugan, E., Soydugan, F., Demircan, O., Ibanoglu, C. (2006). A catalogue of close binaries located in the δ Scuti region of the Cepheid instability strip. Not. R. Astron. Soc., vol. 370, 2013-2014

Uthas, H. (2005). High-Speed Astrophysics: Rapid Events Near compact Binaries. Lund Observatory, Sweden.

Vander Haagen, G.A. (2008). Techniques for the study of high frequency optical phenomena. Proceedings for the 27th Annual Conference of the Society for Astronomical Sciences, 115-122.

Vander Haagen, G.A. (2011). The Silicon Photomultiplier for High Speed Photometry. Proceedings for the 30th Annual Conference of the Society for Astronomical Sciences, 87-96.

Warner, B., Woudt, A. (2008). QPOs in CVs: An executive summary. Dept. of Astronomy, University of Cape Town, South Africa.